NASA/TM-2005-213542

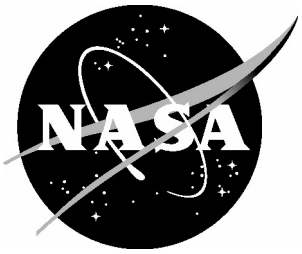

Navier-Stokes Computations of a Wing-Flap Model With Blowing Normal to the Flap Surface

D. Douglas Boyd, Jr.
Langley Research Center, Hampton, Virginia

March 2005

The NASA STI Program Office . . . in Profile

Since its founding, NASA has been dedicated to the advancement of aeronautics and space science. The NASA Scientific and Technical Information (STI) Program Office plays a key part in helping NASA maintain this important role.

The NASA STI Program Office is operated by Langley Research Center, the lead center for NASA's scientific and technical information. The NASA STI Program Office provides access to the NASA STI Database, the largest collection of aeronautical and space science STI in the world. The Program Office is also NASA's institutional mechanism for disseminating the results of its research and development activities. These results are published by NASA in the NASA STI Report Series, which includes the following report types:

- TECHNICAL PUBLICATION. Reports of completed research or a major significant phase of research that present the results of NASA programs and include extensive data or theoretical analysis. Includes compilations of significant scientific and technical data and information deemed to be of continuing reference value. NASA counterpart of peer-reviewed formal professional papers, but having less stringent limitations on manuscript length and extent of graphic presentations.

- TECHNICAL MEMORANDUM. Scientific and technical findings that are preliminary or of specialized interest, e.g., quick release reports, working papers, and bibliographies that contain minimal annotation. Does not contain extensive analysis.

- CONTRACTOR REPORT. Scientific and technical findings by NASA-sponsored contractors and grantees.

- CONFERENCE PUBLICATION. Collected papers from scientific and technical conferences, symposia, seminars, or other meetings sponsored or co-sponsored by NASA.

- SPECIAL PUBLICATION. Scientific, technical, or historical information from NASA programs, projects, and missions, often concerned with subjects having substantial public interest.

- TECHNICAL TRANSLATION. English-language translations of foreign scientific and technical material pertinent to NASA's mission.

Specialized services that complement the STI Program Office's diverse offerings include creating custom thesauri, building customized databases, organizing and publishing research results ... even providing videos.

For more information about the NASA STI Program Office, see the following:

- Access the NASA STI Program Home Page at ***http://www.sti.nasa.gov***

- E-mail your question via the Internet to help@sti.nasa.gov

- Fax your question to the NASA STI Help Desk at (301) 621-0134

- Phone the NASA STI Help Desk at (301) 621-0390

- Write to:
  NASA STI Help Desk
  NASA Center for AeroSpace Information
  7121 Standard Drive
  Hanover, MD 21076-1320

NASA/TM-2005-213542

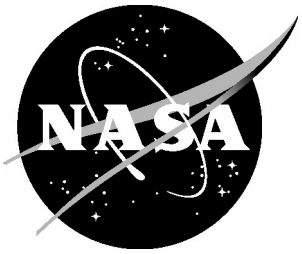

Navier-Stokes Computations of a Wing-Flap Model With Blowing Normal to the Flap Surface

D. Douglas Boyd, Jr.
Langley Research Center, Hampton, Virginia

National Aeronautics and
Space Administration

Langley Research Center
Hampton, Virginia 23681-2199

March 2005

Available from:

NASA Center for AeroSpace Information (CASI)
7121 Standard Drive
Hanover, MD 21076-1320
(301) 621-0390

National Technical Information Service (NTIS)
5285 Port Royal Road
Springfield, VA 22161-2171
(703) 605-6000

Navier-Stokes Computations of a Wing-Flap Model With Blowing Normal to the Flap Surface

D. Douglas Boyd, Jr.

Abstract

A computational study of a generic wing with a half span flap shows the mean flow effects of several blown flap configurations. The effort compares and contrasts the thin-layer, Reynolds averaged, Navier-Stokes solutions of a baseline wing-flap configuration with configurations that have blowing normal to the flap surface through small slits near the flap side edge. Vorticity contours reveal a dual vortex structure at the flap side edge for all cases. The dual vortex merges into a single vortex at approximately the mid-flap chord location. Upper surface blowing reduces the strength of the merged vortex and moves the vortex away from the upper edge. Lower surface blowing thickens the lower shear layer and weakens the merged vortex, but not as much as upper surface blowing. Side surface blowing forces the lower surface vortex farther outboard of the flap edge by effectively increasing the aerodynamic span of the flap. It is seen that there is no global aerodynamic penalty or benefit from the particular blowing configurations examined.

1. Symbols

c_f	flap chord [m]
c_m	main element chord [m]
C_L	wing lift coefficient
C_p	pressure coefficient
C_μ	jet momentum coefficient
a	speed of sound [m/sec]
L	length scale = main element chord [m]
$\dot{m}$	mass flow rate [kg/m^3]
q	order of convergence
p	pressure [N/m^3]
r	grid refinement ratio
x	streamwise coordinate [m]
u	velocity [m/s]
γ	ratio of specific heats
η	non-dimensional spanwise location
ε	fractional error
ρ	density [kg/m^3]
Ω	normalized vorticity magnitude
$(\ldots)_b$	quantities associated with blowing
$(\ldots)_\infty$	freestream quantities

2. Introduction

As engines become quieter, other sources of aircraft noise begin to dominate. An example is the set of non-propulsive sources of aircraft noise collectively known as “airframe noise.” When an aircraft is on approach to an airport with the engines at a low thrust setting and high lift devices deployed, airframe noise appears as a dominant source. Though many airframe noise sources exist, flap side edge noise can be a dominant component. To meet future, tougher FAA standards, reductions will be required in both engine and airframe noise. An understanding of the underlying aerodynamics and aeroacoustics is necessary to provide guidance for noise reduction strategies.

A number of experimental studies in the 1970s were conducted to quantify flap side edge noise. Crighton[1] provides an overview of these early experimental studies. He points out that, while several simplified models of flap side edge noise have been explored in the past, much work is still required to understand fully the phenomena involved and to develop more practical and accurate prediction capabilities. Macaraeg[2] describes recent experimental and computational studies of flap side edge aerodynamics and aeroacoustics. An important paper cited by Macaraeg[2] is a work by Meadows, *et al.*,[3] which presents measured data that identify regions on the flap side edge where important sources of sound are located. Also cited are computational studies[4,6] made in conjunction with recent flap side edge aerodynamic measurements[7]. These computational fluid dynamic (CFD) results for two flap settings (29° and 39°) show that CFD can be used as a tool to aid in understanding of flap side edge aerodynamics and aeroacoustics. Using measured data and predicted CFD results, Brooks, *et al.*[8] presents an analysis of flap edge noise for various flap edge shapes, which shows there are two strong sources of flap side edge noise. One source is the interaction between the side edge vortex on the upper surface of the flap and the

sharp edge on the upper side edge of the flap. Another source is the interaction between the strong shear layer flowing from the bottom surface of the flap and the sharp edge on the lower side edge of the flap.

Because the noise mechanisms presented by Brooks, *et al.*[8] are primarily mean flow aerodynamic flow features interacting with sharp edges, modifying these mean flow features should affect the noise. This paper presents a computational study of the changes made to the mean flow aerodynamic features near the flap side edge when air is blown from small slits, normal to the flap surface, near the flap side edge.

3. Background

Historically, three primary types of blowing configurations have been associated with wings or flaps. These are the "externally blown flap" (EBF), the "internally blown flap" (IBF), and the "wing tip jet" (WTJ). The EBF consists of an arrangement where the flap (and/or wing) is blown by an external jet such as from engine exhaust nozzle. This type of device typically has been studied for lift augmentation of a short take off and landing (STOL) vehicle. The IBF, in the past, has been used to refer to both (1) air blown over the flap from a slit in the trailing edge of a wing and (2) air blown from a slit in the trailing edge of the flap. These, too, have generally been used in the context of lift augmentation of STOL vehicles. In general, the IBF configurations for STOL applications are arranged such that the blowing slit is parallel to the trailing edge of the airfoil.

Unlike the EBF and IBF devices, which typically blow air in a streamwise direction, WTJ devices have typically blown air in a cross-stream direction. Configurations in the literature have blown air (1) in a spanwise direction from slits in the outboard portion of the wing and (2) normal to the wing upper and/or lower surface from small discrete circular jets near the wing tip.

While the introduction in section 2 above provided motivation for using flap blowing, this section examines previous literature associated with EBF, IBF, and WTJ configurations on order to put the current work into context.

3.1. EBF and IBF devices

As far back as 1959, Maglieri, *et al.*[9] examined the noise directivity and frequency spectrum associated with an EBF, where a cold jet was blown past the upper surface of a flap. This work was primarily studied the acoustic effects of turning a jet flow by a flap. They showed that the directivity is affected by the addition of a flap in the nozzle stream and that turning of the jet exhaust causes the noise pattern to be turned by an equal amount. These tests were conducted with jets at large pressure ratios (near choking of the nozzle) with circular and rectangular nozzles. In the 1970s, work associated with EBF configurations was geared toward high lift systems that incorporated "jet augmented lift systems." These systems were examined in an effort to develop the lift necessary for short take off and landing (STOL) aircraft. This led to many acoustic studies on these devices in order to understand, and eventually reduce, the noise generated. Typically, these configurations employed very high pressure ratio nozzle systems for augmenting the lift on the wing or flap.

Dorsch, *et al.*[10] examined the acoustic characteristics of EBF configurations, starting in the early 1970s. They included EBF configurations and a "wing augmentor" flap. They concluded that both of these implementations "will present serious noise problems." Gibson[11] also made measurements for an EBF configurations, including wing augmentor flaps and internal blowing over the flaps from the wing trailing edge. Several slot configurations at the wing trailing edge were examined. He found that the internally blown configuration (*i.e.*, air blown from the wing trailing edge over the flap) was quieter than the other configurations. McKinzie, *et al.*[12] measured the EBF and wing augmentor noise characteristics of a STOL configuration, with the addition of a secondary blowing system at the trailing edge of the flap. Though many configurations were examined, only limited overall sound pressure measure-

ments were made for each configuration. These measurements showed that some of the configurations reduced noise while others increased it.

Clark, *et al.*[13] developed an empirical noise prediction capability for EBF configurations based on previous experimental studies. They concluded that this capability provided "acceptable preliminary results for configurations similar to those contained in the analysis." Simultaneously, Fink[14] examined noise mechanisms from existing literature, combined them with known flow properties, and developed a noise prediction capability for an EBF configuration on a component-by-component basis. His results compare favorably to measured data.

Parker, *et al.*[15] used an IBF device, blowing air from the trailing edge of the flap using "bleed" air from the engine, to study its effect on transonic maneuverability of two fighter aircraft. When resizing the aircraft to account for the maneuverability and performance changes, it was found that the IBF system provided a maneuverability and performance design benefit for the "interdiction" aircraft. However, due to the additional weight of the IBF system needed to provide appropriate blowing for the "air superiority" aircraft, the IBF system was deemed a design penalty for the "air superiority" aircraft.

Falarski, *et al.*[16] examined several configurations, including an over-the-wing EBF, and under-the-wing EBF, an IBF, and an augmentor wing. They examined the effects of forward speed and found only a low frequency, 2dB reduction for two of the configurations in an 80 knot freestream. They summarized the noise characteristics of all of the configurations, but indicated that all configurations are 10 to 15 PNdB higher than the noise goal of 95 PNdB.

In a more fundamental EBF study, Reddy, *et al.*[17] examined the acoustic characteristics of a circular jet impinging on an isolated flap. The variations in acoustic power, directivity, *etc.* were measured as a function of jet exit Mach number and flap length. Both a "short flap" configuration and a "long flap" configuration were examined. As discussed above, previous experiments used configurations where the pressure ratio was near the nozzle choking condition (*i.e.*, the nozzle exit Mach number is near unity). In this study, the jet exit Mach number varied from the near-choking condition to an exit Mach number of 0.3. Reddy, *et al.*[17] concluded that the dominant source of noise for the short flap configuration is the "interaction between the flow turbulence and the flap trailing edge." They also concluded that the dominant noise mechanism for the long flap configuration is the "Reynolds fluctuating stresses similar to those in a free jet but modified by the presence of the surface."

McKinzie, *et al.*[18] examined several noise reduction concepts for EBF configurations in conjunction with several IBF configurations. The EBF/IBF configuration was a three element airfoil (consisting of a wing and two flaps) similar to McKinzie, *et al.*,[12] but included partial covers for the gap between the wing and flaps and jet Mach numbers from approximately 0.5 to 0.8. From this study, they concluded there are three main noise sources for these configurations. These sources are (1) the jet impact on the surface, (2) the fluctuating lift response due to the jet inflow over the wing, and (3) the trailing edge noise from the second flap. In a companion paper, Burns, *et al.*[19] examined a large number of blown flap configurations with multiple flap elements. The variations of these configurations included perforated flap surfaces and perforated screens. The perforated screens were found to reduce noise more that the perforated surface, but no configuration was effective in reducing noise over the entire frequency range for the velocities examined.

Gibson[20] provides a brief review of work on determination of noise source characteristics and noise reduction concepts for EBF configurations prior to 1976.

Vogler[21] examined the effect of an IBF device, blowing air over the flap from slits near the trailing edge of the main wing, on the low speed longitudinal characteristics of a STOL aircraft. He found that higher lift coefficients could be reached when blowing is used over the entire span of the flap rather than a partial span.

Pennock[22] took acoustic measurements of an EBF configuration with jet Mach numbers ranging from 0.5 to 0.72, but also included the effects of forward speed up to 80 knots. He also examined modifications to the flap system of the multi-element airfoil, such as changing the third flap from a solid to a

perforated surface. In this work, he derived a simple formula for the change in sound pressure level as a function of the jet velocity, the forward velocity, and an exponent of the "relative velocity ratio".

McKinzie[23] examined noise suppression devices on EBF configurations for multi-element wings (with a main element and multiple flaps) and their aerodynamic penalties. He found that decreased distance between the nozzle and the second flap reduced the broadband noise in the approach configuration, while flap-gap fairings (*i.e.*, fairings covering the gap between the flaps) and flap screens reduced high frequency noise. Aerodynamically, the flap-gap fairing configuration had the lowest performance penalty.

Reddy[24] performed a comparison of circa 1978 analytical models associated with EBF noise prediction. After comparing predicted overall sound pressure levels, directivity, and spectra with measured data, he identified a number of items that needed further investigation to improve predictive models. For example, he points out that investigations of the turbulence characteristics of flow around flaps are needed. In addition, he states that investigations of flow inhomogeneities near a surface, and their effect on noise generation and propagation, are needed. He also provided an extensive bibliography of flap noise research, circa 1978.

In 1984, a novel STOL concept using an internal wing blowing technique, was investigated by Krothapalli, *et al.*[25] In this experimental investigation, which was designed to explore the physical aspects of this device, they examined a wing with a narrow blowing slit oriented parallel to the trailing edge, but located at mid-chord on the lower surface of the airfoil. Air was blown normal to the airfoil surface and was found to have a profound effect on the wing pressure coefficient distribution. They found that for angles of attack below stall, the lift coefficient exhibits behavior similar to a jet-flap configuration.

3.2. WTJ devices

The previous section outlined in detail previous work on externally and internally blown flaps and wings. These focused almost exclusively (with the exception of Krothapalli, *et al.*[25]) on blowing in the streamwise direction from either an external jet nozzle or from slits parallel to the wing or flap trailing edge. This section examines devices in which the flow issues from slits or jets at or near the wing tip, but in a cross flow direction.

In the 1960s, Spreemann[26] examined the freestream interference effects of roll control jets that were located near the tip on the underside of a swept wing. These effects were examined for a vertical take off and landing (VTOL) aircraft model. He found that the interference effects from these jets were detrimental to roll control and that aileron deflection had little effect on the interference effects.

Scheiman, *et al.*[27] modified the wing tip of a semi-span model several ways in an attempt to modify the tip vortex properties downstream of the tip. One of the modifications used a wing tip slit, parallel to the chord, to blow air spanwise outward from the tip. This slit in the wing tip was very narrow, covered nearly the entire chord length, and could blow air at several angles relative to the spanwise direction. The wing tip blowing examined had no measurable effect on the tip vortex location or vortex core cross-sectional properties downstream of the wing. In an effort to reduce the drag on a wing, Shipman, *et al.*[28] examined blowing from long, thin chordwise slits located near the wing tip. Various slits were located such that blowing could occur either spanwise from the wing tip, normal to the chord on the upper surface, or normal to the chord on the lower surface. They found that spanwise blowing produced an increase in wing efficiency and that a 15% overall decrease in drag could be attained. A substantial movement of the downstream tip vortex was also measured. The difference in the tip vortex motion conclusions between Scheiman, *et al.*[27] and Shipman, *et al.*[28] can be attributed to the fact that Shipman, *et al.*[28] used blowing that ranged between 8 and 36 times stronger than Scheiman, *et al.*[27]. Tanaka, *et al.*[29] examined the effects of wing tip jets (oriented chordwise) on the decay of a tip vortex. They found that the total circulation in the tip vortex is not reduced when tip jets are used, but the tip vortex "filaments" are spread over a larger region.

Wu, *et al.*[30,31] also used chordwise wing tip slits in an attempt to improve wing aerodynamics. Whereas previous studies used slits with lengths on the order of the chord length, this study used "discrete jets" for the first time. The discrete jets are very short in length and are on the order of 20% of the chord length. Multiple jets are located along the wing tip chord and are blown in various directions, which include various dihedral and sweep angles relative to the spanwise direction. Blowing occurred at low to moderate strengths. They examined low speed (freestream Mach number of 0.06) and very low aspect ratio conditions and concluded that the jets had an effect on the spanwise pressure distribution and that multiple additional vortex systems can be generated by these cross flow jets.

Tavella, *et al.*[32] examined experimentally a low aspect ratio wing in a low speed freestream with strong blowing from chordwise slits in the wing tip. These slits were nearly the length of the wing tip chord. They found that the lift distribution on the entire wing was affected. They summarized that the increase in lift and performance was due to an effective increase in wing span and that this mechanism can induce aerodynamic moments that can be used for roll and lateral control of aircraft. In a series of companion papers, Tavella, *et al.*[33,34,35] developed an analytical relation between the blowing and aerodynamic forces.

Smith, *et al.*[36] performed flow visualization in a water tunnel using a swept wing with two wing tip jets. Various jet lengths were used with various jet-sweep and dihedral angles. Also varied was the wing angle of attack and the blowing intensity. They showed that the jet entrains flow from the upper surface and carries it outboard of the wing tip. For data reduction purposes, a "jet span" was defined as "the span of the wing plus the spanwise extent of the jet." For a given blowing momentum coefficient, they found that both the large jets and small jets increase the "jet span" by the same amount. In a greatly expanded version of the work presented in Smith, *et al.*,[36] Mineck[37] provided a comprehensive analytical and experimental investigation of blowing from wing tip jets for a moderate aspect ratio swept wing. A number of configurations of multiple blowing slits were used over a range of blowing strengths. These measurements were complemented by flow visualizations in a water tunnel and by Navier-Stokes computations of the effects of blowing at higher Mach numbers. This work finds that this particular blowing technique can slightly reduce drag while slightly increasing lift at lower Mach numbers, but causes increased drag at higher Mach numbers.

3.3. Current configuration

The previous sections provided a detailed list of prior experimental and analytical work in the area of wing and/or flap blowing. To recapitulate, there have been two primary focus areas in previous literature. One has been the use of external wing and/or flap blowing to augment lift of STOL aircraft. Internal blowing, if used, incorporated slits that are parallel to the wing or flap trailing edge. The second focus area has been wing tip slits blowing primarily in the spanwise direction in an attempt to either increase lift or decrease drag.

The current configurations consist of small, short slits ("discrete jets") that run chordwise near the flap side edge on either the upper surface, the lower surface, or the flap side face. These discrete jets blow normal to the flap surface. This appears to be the first analytical examination of flap jets in these orientations. In addition, because only a local mean flow aerodynamic effect on the upper surface vortex or the lower surface shear layer is desired (as described in section 2 above), jet momentum coefficients that are an order of magnitude below any previous examinations are considered.

4. Geometry

The baseline configuration with no blowing is composed of a NACA 63_2-215 Mod B wing with a 30% chord, half-span, Fowler flap. The reference chord for the previous description is taken to be the main element chord on the portion of the span without the flap. Figure 1 shows the baseline geometry with the wind-tunnel walls excluded for clarity. In this figure, a "close-up" region is marked for later

reference for figures 2, 3, and 4. The portion of the main element upstream of the flap contains a half-span, lower surface flap cove and a half-span, trailing edge cut-out. The baseline configuration is set at an angle of attack of 10° in the tunnel. The wind-tunnel walls are included in the computation as inviscid surfaces. This configuration corresponds to the 29° flap "7x10 geometry" examined by Khorrami, *et al.*[5,6] The configurations with blowing are identical to the baseline case, except they each contain a small slit near the flap side edge. These slits are used to blow air normal to the flap surface from a constant pressure plenum that is internal to the flap.

Three blowing configurations (labeled configurations 1, 2, and 3) are examined. The first configuration consists of an slit on the upper surface of the flap near the side edge. Figure 2 shows this configuration with the blowing slit as a black strip on the flap surface. The second configuration, shown in figure 3, has a blowing slit on the lower surface. Note that in figure 3, the flap side edge has been removed so that the lower flap surface and slit location can be seen. The third configuration blows from a slit on the flap side edge as seen figure 4. Table 1 contains the locations of the leading edge and trailing edge of each of the slits as well as the width of the slot for the three configurations. For configurations 1 and 2, the side of the slit is 0.83%c_f inboard of the flap edge. For configuration 3, the slit is parallel to, and 3.12%c_f above, the flap chord line. In addition, the table lists the pressure (p_b), velocity (u_b), and density(ρ_b) used at the blowing slits for these configurations. The conditions listed are normalized per the CFL3D reference manual[38].

Table 1: Slit Leading Edge and Trailing Edge Locations, Width [%c_f], and Blowing Conditions

Configuration	L.E. [%c_f]	T.E. [%c_f]	width [%c_f]	$\frac{p_b}{\gamma p_\infty}$	$\frac{u_b}{a_\infty}$	$\frac{\rho_b}{\rho_\infty}$
1	50.0	75.0	1.67	0.7166	0.075	0.9814
2	27.0	60.0	1.67	0.7166	0.075	0.9814
3	27.0	60.0	1.67	0.7166	0.075	0.9814

For all cases, the freestream Mach number is 0.20 and the Reynolds number (referenced to the main element chord) is 3.7 million. Note from table 1 that the pressure applied at the blowing slit is slightly above the freestream static pressure, the blowing Mach number (u_b/a_∞) normal to the surface is three-eighths of the freestream Mach number, and the density applied at the blowing slit is slightly below the freestream density. To relate the blowing intensity to previous literature, the jet momentum coefficient is introduced here and is defined as:

$$C_\mu = \frac{\dot{m}_b u_b}{\frac{1}{2}\rho_\infty u_\infty^2 c_m^2} \tag{1}$$

Previous literature discussed above examined jet momentum coefficients the approximate range $0.001 < C_\mu < 0.27$. Here, a value of $C_\mu \approx 0.0001$ is used, which is an order of magnitude lower than prior work. It is anticipated that these small slits with very small jet momentum coefficients will affect the upper surface vortex or the lower surface shear layer without adversely adding a new, detrimental source of noise. In this study, only the aerodynamic effects of the jets are examined; the quantitative acoustic effects are beyond the scope of the present paper.

5. Computational Method

For computations here, the thin-layer, Reynolds-averaged, Navier-Stokes (RANS) equations are solved in curvilinear coordinates using CFL3D (version 6)[38]. This structured grid, finite volume, RANS

solver uses a third-order, upwind-biased, spatial discretization scheme for the convection and pressure terms and a central-difference spatial discretization scheme for the shear stress and heat transfer terms. Implicit time advancement using three-factor approximate factorization and local time stepping is used in conjunction with multigrid and mesh sequencing for convergence acceleration. Numerous turbulence models are available in CFL3D, but the Spalart-Allmaras one-equation model is used exclusively in this study and the flow is assumed to be fully turbulent.

The computational grid consists of approximately 4.2 million grid points distributed amongst 16 grid domains that are connected by either 1-1 blocking or patched interfaces. The main element and flap surfaces are modeled as viscous, adiabatic walls. The wind-tunnel walls are modeled as inviscid surfaces. The wind-tunnel inflow and outflow planes are both modeled with characteristic inflow/outflow boundary conditions.

For purposes of this paper, CFL3D was modified to include a boundary condition where plenum conditions could be specified at the blowing surface slit. CFL3D originally used an additional surface velocity to model surface blowing. To accomplish this, once the surface velocities were set to zero on the cell face in the viscous surface model, an additional user-specified velocity was added normal to the surface. The surface pressure was computed internally by extrapolating from the flowfield, then the density at the surface was computed using the extrapolated pressure and the speed of sound at the surface. Because the pressure is extrapolated from the flowfield, a pressurized plenum could not be modeled using the original blowing boundary condition. For this paper, to model blowing with an internal pressurized plenum, a new boundary condition was implemented. A schematic for this boundary condition is shown in figure 5. This figure shows a surface and the computational domain outside the surface. Also seen are the boundary cells, or "ghost" cells, which CFL3D uses to specify cell center-type boundary conditions. For this new boundary condition, at these cell centers, an user-specified pressure, blowing velocity, and density are applied. The blowing velocity is assumed to be normal to the surface at the ghost cell centers. For the cases studied here, the user-specified values of pressure, blowing velocity, and density are given in table 1.

6. Convergence

6.1. Solution Convergence

Grid sequencing (using grid doubling) involving three grid refinements was performed in the process of obtaining a solution on the finest grid for all cases. Here, the lift coefficient is used as the primary indicator of convergence. The lift coefficient, and therefore the solution, was considered to be converged when the following criterion was met:

$$\left|\frac{dC_L}{dN}\right| \le 0.01\% \tag{2}$$

where N is the iteration number. Typically, this level of convergence was obtained at approximately 4900 fine grid iterations. Each converged solution required approximately 290 CPU hours on a Compaq Alpha XP1000 Workstation containing a single, 667 MHz, Alpha EV6.7 (21264A) processor. Each case used approximately 1.45Gb of the 2.00 Gb installed memory.

6.2. Grid Convergence

To demonstrate the level of grid convergence for the baseline case, the converged lift coefficients on the medium grid and the fine grid are used to compute a Grid Convergence Index[39] (GCI) for the fine grid solution. The coarse grid solution is not included in the computation of the GCI because it is well outside the "asymptotic range," as described Roach[39]. The fine grid GCI (or, "GCI[fine]") provides an

estimate of a "reasonable error band" on the solution (*i.e.*, lift coefficient) on the fine grid and is defined as follows:

$$\mathrm{GCI[fine]} = \frac{F_s|\varepsilon|}{r^q - 1} \tag{3}$$

where the F_s is the "factor of safety" ($F_s = 3$), r is the grid refinement ratio ($r = 2$), q is the convergence rate. Because a third order accurate method is used, it is assumed that $q = 3$. This value of q is optimistic and is justification for the usage of the factor of safety value given above. For this paper, the fractional error estimate, ε, is based on the total lift coefficient and defined as follows:

$$\varepsilon = \frac{C_L^{medium} - C_L^{fine}}{C_L^{fine}}. \tag{4}$$

For the baseline case, the converged lift coefficient for the medium grid is 2.244 and for fine grid is 2.342. Based on these values, the value of GCI[fine] = 1.8%, which means that the estimated "reasonable error band" on the computed converged fine grid lift coefficient is ± 0.042. Similar GCI values are obtained for the blowing cases. These similarities result from the fact that the blowing cases are effectively perturbations of the baseline because of the small blowing area and the very low blowing velocities.

7. Results and Discussion

7.1. Baseline vorticity

Figure 6 shows a close up view of the flap side edge for the baseline (no blowing) configuration. The slices shown are in planes normal to the flap chord line at several chordwise stations. The contours on these slices are of the magnitude of the normalized vorticity component normal to the slice. For all figures shown, the vorticity magnitude, Ω, is normalized by L/a_∞. Here, the length scale, L, is the main element chord and a_∞ is the freestream speed of sound. This view clearly illustrates two vortex structures generated on the forward portions of the flap at the sharp upper and lower edges. It is also seen that the vortex from the lower surface rolls onto the top surface at approximately the mid-chord of the flap. This vortex suppresses, then merges with, the vortex generated on the upper surface. Downstream of this merger, the merged vortex separates from the upper surface of the flap while continuing to be "fed" from the strong shear layer flow from the lower surface.

Predictions of this dual vortex structure have been shown previously and compared to experimental results by Khorrami, *et al.*[5,6] In addition, Brooks, *et al.*[8] demonstrated that two dominant noise sources from this configuration are from (1) the merged upper vortex interacting with the upper sharp edge of the flap side edge, and (2) the strong shear layer flowing across, and interacting with, the lower sharp side edge. This dual vortex structure is not unique to flap side edge flows. This flow characteristic is a feature of flat wing tips with sharp edges, as demonstrated by Anderson, *et al.*[40]

7.2. Dual vortex structure

As discussed above, a dual vortex structure is seen on forward portion of the flap side edge; one vortex forms on the upper surface and one vortex forms on the lower vortex. This dual vortex structure is a flow feature of wing tips with flat side faces, as shown by Anderson, *et al.*[40] and Francis, *et al.*[41] Discussions of the dual vortex structures in references 5, 40, and 41 have focused on the lower surface vor-

tex and have stated that this vortex is due to flow separation at the lower flap edge. Further investigation of the flowfield computations reveals more detail about the formation of the side edge vortices.

Figure 7(a) shows streamlines in the region near the nose of the flap. As the flow approaches the flap nose from upstream, a very strong spanwise flow is induced by the presence of the flap surface. When this spanwise flow travels outboard along the front of the flap nose, it encounters the edge of the flap. In this small region, the flow traveling over the side edge of the flap is analogous to the flow over a backward-facing step. As expected from a backward-facing step, the flow separates at the edge and generates a horseshoe vortex. The reverse flow seen in "region 1" of figure 7(b) is further evidence of this horseshoe vortex. This horseshoe vortex is "bent" downstream by the prevailing flow near the side edge of the flap. The lower branch of this horseshoe vortex travels streamwise along the flap side edge and generates a downward flow at the flap side surface; this feature is seen in "region 2" of figure 7(b). Ultimately, this lower vortex branch separates from the upper flap surface at approximately the mid-chord of the flap.

The upper branch of the horseshoe vortex travels along the upper surface until the low pressure region on the suction side of the flap forces it to separate from the flap. However, this upper branch of the horseshoe vortex is not the upper surface vortex seen in figure 6. The generation of the upper surface vortex in figure 6 can be explained by further examination of figure 7(a). The strong horseshoe vortex in figure 7(a) acts as if it were a "tube" sitting on the flap side surface. In this case, the "tube" is formed as a fluid structure (vortex) rather than as a structural protrusion of the flap. As flow travels over this fluid "tube," it reattaches to the side surface in region 3 and follows the prevailing local freestream. (For clarity, the forward parts of the streamlines in region 3 have been truncated.) The streamlines in region 3 pass over the upper surface and separate from it at the edge. As with a backward facing step, the flow over the upper surface edge in region 3 separates and forms another horseshoe vortex. This upper surface horseshoe vortex is the upper surface vortex seen in figure 6.

7.3. Top blowing vorticity

As discussed above, several configurations that use blowing normal to the flap surface, near the flap side edge, are explored as possible methods to affect the interactions of the shear layer with the lower side edge or the upper surface vortex with the upper side edge. The first configuration examined here is one that employs blowing from a slit on the top surface of the flap near, and parallel to, the side edge. The slit location is seen in figure 2 and the geometry has been described in an earlier section. To have maximum impact on the merged vortex, the slit location has been chosen to correspond to the location where the merged vortex "rolls" over the top surface.

In a manner similar to figure 6, figure 8 illustrates the normalized vorticity magnitude in planes normal to the flap chord line for the top blowing configuration (*i.e.*, configuration 1). Comparing figures 6 and 8, the flow features on the forward portion of the flap are very similar. These features, consisting of the dual vortex formation, near the nose are similar to the baseline and are described in detail above in section 7.2. The blowing affects only the flowfield near, and downstream of, the blowing slit. This is an expected result due to the low blowing velocities and small blowing surface area.

The effects of the upper surface blowing on the flowfield begin at the forward extent of the blowing slit. The merger of the upper and lower vortices seen in the baseline case is delayed until further downstream. The merging vortex system is split into two parts by the (relatively) high pressure, low-velocity jet of air from the blowing orifice. This results in a weaker and more diffuse vortex downstream of the slit. In addition, starting at the slit, interaction of the merged vortex with the upper sharp edge is nearly eliminated by splitting the system into a shear layer outboard of the jet and a weaker vortex inboard of the side edge. This suggests that the top blowing configuration may be effective in reducing the noise associated with the upper surface vortex interaction with the sharp upper edge of the flap. It also suggests that this configuration will have little effect on the noise associated with the lower surface shear layer interaction with the lower flap side edge.

7.4. Bottom blowing vorticity

The second configuration examined here is one that employs blowing from a slit on the lower surface of the flap near, and parallel to, the side edge. The slit location is seen in figure 3 and the geometry has been described in an earlier section. In this case, the slit location has been chosen to correspond to the location on the lower surface where the shear layer begins to "feed" the vortex that ultimately spills over onto the upper surface.

Figure 9 shows the vorticity contours for the bottom blowing configuration computation. In this case, the lower shear layer is thickened at the blowing location relative to the baseline and configuration 1 cases. The thickened shear layer near the blowing slit appears to be translated slightly downward, away from the lower surface side edge. This deformation of the shear layer causes it to travel with a slightly larger radius of curvature around, and thus slightly farther away from, the flap side. Whereas the merged vortex topology and vorticity distribution in configuration 1 is substantially different from the baseline, figure 9 shows that the configuration 2 merged vortex topology is very similar to the baseline case, while the maximum vorticity is slightly lower. Relative to the baseline, the reduction in vortex strength for configuration 2 is less than that for configuration 1. Because this configuration affects primarily the lower shear layer, the computations suggest that this bottom blowing configuration will affect the shear layer noise component, but have little effect on the noise from the upper surface vortex interaction with the upper flap edge.

7.5. Side blowing vorticity

The third configuration examined employs blowing from a slit on the flat side surface of the flap parallel to, and above, the flap chord line. The slit location is seen in figure 4 and the geometry has been described in an earlier section. In this case, the slit location has been chosen to aerodynamically increase the effective span of the flap and thus push the lower surface vortex spanwise away from the flap edge.

Figure 10 illustrates the vorticity contours of the side blowing computations. As with previous cases, the forward portion of the flowfield is similar to the baseline and contains the dual vortex structure seen in all previous cases. However, examination of the flowfield around the side of the flap reveals that blowing through the side surface appears to disrupt the vorticity distribution more than either the top or bottom blowing cases. An example of this disruption can be seen by comparing the third slice from the front of the flap in figures 6, 9, and 10. In the third slice in figure 10, the lower vortex is pushed farther outboard of the flap side edge. The injection of low velocity, (relatively) high pressure air from the blowing slot also weakens the lower surface vortex as it starts to roll up over the top surface. As with the top blowing configuration, side blowing appears to primarily affect the upper surface vortex interaction with the upper flap edge. As such, the upper vortex component of the noise is expected to be affected and the shear layer component is expected to see little effect.

7.6. Detailed vorticity

The previous sections provided a qualitative examination of the effect of blowing on vorticity and vortex positioning. This section provides a quantitative look at these effects.

Figure 6, as discussed above, shows the vorticity contours for the baseline case. Also shown on the figure is a location (labeled "A") where further detail will be discussed. Location "A" is chosen so that it (1) is in the plane of the fourth slice in figure 6, and (2) cuts through the center of the vortex on the fourth slice. This particular slice is chosen because previous literature[3,8] has shown that this vortex is at the root of the noise source near the mid-chord of the flap. Figures 8, 9, and 10 show similar locations labeled B, C, and D, respectively. Note that locations A, B, C, and D are co-linear so that the vorticity can be examined at the same location in space for the various configurations.

Figure 11 shows the normalized vorticity magnitude for locations A, B, C, and D. The horizontal axis depicts the spanwise location, normalized by the main element chord, relative to the flap side edge. The flap side edge corresponds to the origin on the horizontal axis. Positive values (to the left) are for locations inboard of the flap side edge; negative values (to the right) are for locations outboard of the flap side edge. The vertical axis is the normalized vorticity magnitude normal to the plane of the slice. The scale on the vertical axis corresponds to the same range used in figures 6, 8, 9, and 10.

For the baseline case (location A) the vorticity reaches a maximum above the flap side edge and decays rapidly, and nearly symmetrically, on either side of the maximum value. Using top blowing (location B), the maximum vorticity peak has been reduced by an approximately 20% relative to the baseline case and the vorticity distribution is no longer symmetric. Bottom blowing (location C) causes the vorticity distribution to retain the same general shape as the baseline case, but with approximately 20% reduction in the maximum value and a slight outboard shift. Side blowing (location D) has the largest effect on the vorticity distribution of the cases examined so far. Location D shows that (1) the maximum vorticity magnitude has been reduced nearly 40% relative to the baseline maximum, (2) the peak has been shifted outboard of the side edge, and (3) the vorticity is nearly constant across the center portion of the vortex between the spanwise locations from 0 to -0.015.

7.7. Effects on aerodynamic performance

In the previous section blowing was shown to affect the vorticity distribution in a local manner. However, preferably these effects do not adversely affect the global aerodynamics of the system. This section will show that the global aerodynamics are nearly unaffected by the addition of the blowing aerodynamics in these cases.

To relate the current work to previous literature, the pressure coefficient is presented in figure 12. This figure provides the pressure coefficients at the same spanwise locations as shown in figure 9 of Takallu, *et al.*[4] Comparing current predictions (figure 12) to previous predictions (figure 9 of Takallu, *et al.*[4]), it is seen that current predictions are consistent with previous literature[4]. Plots in figure 12 provide a global picture of the aerodynamic characteristics of the main element and flap system. As seen in the discussions of the vorticity distributions previously, the effects of the blowing on the aerodynamics are localized to regions near the blowing slits. This fact is reflected in the pressure coefficient distributions for the blowing cases. The changes in the global pressure coefficient distributions are minuscule for the blowing cases (compared to the baseline case seen in figure 12), and therefore not shown here.

This global similarity also has been discussed above in the context of the GCI. Earlier, the GCI was used to show the global grid convergence characteristics related to the lift coefficient for the entire wing/flap system. In fact, the top and bottom blowing cases had virtually identical lift coefficients. The side blowing case exhibited a very small increase of 0.17% in the overall lift coefficient. This finding is consistent with previous literature where the effective aerodynamic span was increased (this increasing the lift) by spanwise blowing. Based on these findings, for these particular blowing configurations, we infer that is no global aerodynamic performance penalty (or benefit) is incurred from such as system.

8. Conclusions

A Navier-Stokes solver has been used to study the aerodynamic effects of flap side edge blowing for three blowing configurations. This is the first known computational study of blowing from configurations such as this on a flap. Grid convergence was demonstrated. A new “plenum blowing” boundary condition was introduced to model the plenum pressure, density, and blowing velocity. For all three blowing configurations, the maximum vorticity peak was reduced relative to the baseline in the vicinity of the upper surface noise source. Of these three configurations, the side blowing configuration produced the largest reduction in vorticity magnitude and moved the peak outboard of the flap side edge. No global aerodynamic penalty (or benefit) is incurred for these blowing configurations.

9. Acknowledgements

The author would like to thank Dr. Florence Hutcheson and Dr. Thomas Brooks for information about the flap blowing configurations. In addition, the author would like to thank Dr. Mehdi Khorrami for providing the baseline computational grid and for many helpful discussions on this topic. This work was performed under the NASA QAT Program.

10. References

1. Crighton, D.G.: *Aeroacoustics of Flight Vehicles: Theory and Practice, Volume 1: Noise Sources*, NASA RP-1258, Vol. 1, Chapter 7, August 1991.

2. Macaraeg, M.G.: *Fundamental Investigations of Airframe Noise*, AIAA Paper 98-2224.

3. Meadows, K.R., Brooks, T.F., Humphreys, W.M., Hunter, W.M., Gerhold, C.H.: *Aeroacoustic Measurements of a Wing-Flap Configuration*, AIAA Paper 97-1595, 3rd AIAA/CEAS Aeroacoustics Conference, Atlanta, GA, May 1997.

4. Takallu, M.A., Laflin, K.R.: *Reynolds Averaged Navier Stokes Simulations of Two Partial Span Flap Wing Experiments*, AIAA Paper 98-0701, 36th Aerospace Sciences Meeting, Reno, NV, January 12-15, 1998.

5. Khorrami, M.R., Singer, B.A., Takallu, M.A.: *Analysis of Flap Side Edge Flowfield for Identification and Modeling of Possible Noise Sources*, SAE Paper 971917, Proceedings of the 1997 Noise and Vibration Conference, Vol. 1, 1997, pp 379-385.

6. Khorrami, M.R., Singer, B.A., Radeztsky, Jr., R.H.: *Reynolds Averaged Navier Stokes Computations of a Flap Side Edge Flow Field*, AIAA Paper 98-0768, 36th Aerospace Sciences Meeting, Reno, NV, January 12-15, 1998.

7. Radeztsky, Jr., R.H., Singer, B.A., Khorrami, M.R.: *Detailed Measurements of a Flap Side Edge Flow Field*, AIAA Paper 98-0700, 36th Aerospace Sciences Meeting, Reno, NV, January 12-15, 1998.

8. Brooks, T.F., Humphreys, W.M.: *Flap Edge Aeroacoustic Measurements and Predictions*, AIAA Paper 2000-1975, 6th AIAA/CEAS Aeroacoustics Conference, Hahaina, HI, June 12-14, 2000.

9. Maglieri, D.J., Hubbard, H.: *Preliminary Measurements of the Noise Characteristics of Some Jet-Augmented-Flap Configurations*, NASA Memorandum 12-4-58L, January 1959.

10. Dorsch, R.G., Krejsa, E.A., Olsen, W.A.: *Blown Flap Research*, AIAA Paper 71-745, AIAA/SAE 7th Propulsion Joint Specialist Conference, Salt Lake City, UT, June 14-18, 1971.

11. Gibson, F.W.: *Noise Measurements of Model Jet-Augmented Lift Systems*, NASA TN D-6710, April 1972.

12. McKinzie, Jr., D.J., Burns, R.J.: *Externally Blown Flap Trailing Edge Noise Reduction By Slot Blowing - A Preliminary Study*, AIAA Paper 73-245, AIAA 11th Aerospace Sciences Meeting, Washington, D.C., January 10-12, 1973.

13. Clark, B.J., Dorsch, R.G., Reshotko, M.: *Flap Noise Prediction Method for a Powered Lift System*, AIAA Paper 73-1028, AIAA Aero-Acoustics Conference, Seattle, WA, October 15-17, 1973.

14. Fink, M.R.: *Mechanisms of Externally Blown Flap Noise*, AIAA Paper 73-1029, J., Dorsch, R.G., Reshotko, M.: *Flap Noise Prediction Method for a Powered Lift System*, AIAA Paper 73-1028, AIAA Aero-Acoustics Conference, Seattle, WA, October 15-17, 1973.

15. Parker, J.L., Ball, R.F.: *An Analysis of the Effects of Internally Blown Jet Flaps on an Advanced Fighter Aircraft Design*, AIAA Paper 74-970, AIAA 6th Aircraft Design, Flight Test and Operations Meeting, Los Angeles, CA, August 12-14, 1974.

16. Falarski, M.D., Aiken, T.N., Aoyagi, K., Koenig, D.: *Comparison of the Acoustic Characteristics of Large-Scale Models of Several Propulsive-Lift Concepts*, AIAA Paper 74-1094, AIAA/SAE 10th Propulsive Conference, San Diego, CA, October 21-23, 1974.

17.Reddy, N.N., Yu, J.C.: *Radiated Noise From an Externally Blown Flap*, NASA TN D-7908, July 1975.

18.McKinzie, Jr., D.J., Burns, R.J., Wagner, J.M.: *Noise Reduction Tests of Large-Scale-Model Externally Blown Flap Using Trailing-Edge Blowing and Partial Flap Slot Covering*, NASA TM X-3379, April 1976.

19.Burns, R.J., McKinzie, Jr., Wagner, J.M.: *Effects of Perforated Flap Surfaces and Screens on Acoustics of a Large Externally Blown Flap Model*, NASA TM X-3335, April 1976.

20.Gibson, J.S.: *New Developments in Blown Flap Noise Technology*, NASA CR-145086, 10th Congress of ICAS, Ottawa, Canada, October 3-8, 1976.

21.Vogler, R.D.: *Wind-Tunnel Investigation of Internally Blown Jet-Flap STOL Airplane Model*, NASA TN D-8309, November 1976.

22.Pennock, A.P.: *Forward Speed Effects on Blown Flap Noise*, AIAA Paper 77-1315, AIAA 4th Aeroacoustics Conference, Atlanta, GA, October 3-5, 1977.

23.McKinzie, Jr., D.J.: *EBF Noise Suppression and Aerodynamic Penalties*, AIAA Paper 78-240, AIAA 16th Aerospace Sciences Meeting, Huntsville, AL, January 16-18, 1978.

24.Reddy, N.N.: *Blown Flap Noise Prediction*, NASA CR-158978, September 1978.

25.Krothapalli, A., Leopold, D.: *A Study of Flow Past an Airfoil with jet Issuing from its Lower Surface*, NASA CR-166610, June 1984.

26.Spreemann, K.P.: *Free-Stream Interference Effects on Effectiveness of Control Jets Near the Wing Tip of a VTOL Aircraft Model*, NASA TN D-4084, August 1967.

27.Scheiman, J., Shivers, J.P.: *Exploratory Investigations of the Structure of the Tip Vortex of a Semispan Wing for Several Wing-Tip Modifications*, NASA TN D-6101, February 1971.

28.Shipman, K.W., White, Jr., R.P., Balcerak, J.C.: *Drag Reduction of a Lifting Surface by Alteration of the Forming Tip Vortex*, Rochester Applied Science Associates, Inc. (RASA) Report 74-06, 1974.

29.Tanaka, S., Kaibara, M., Tanaka, A.: *Decay and Modification of Trailing Vortex*, Bulletin of the JSME, Vol. 21, No. 151, January 1978, pp 98-103.

30.Wu, J.M., Vakili, A.D.: *Aerodynamic Improvements by Discrete Wing Tip Jets*, AFWAL-TR-84-3009, Final Report, March 1984.

31.Wu, J.M., Vakili, A.D., Gilliam, F.T.: *Aerodynamic Interactions of Wingtip Flow with Discrete Wingtip Jets*, AIAA Paper 84-2206, AIAA 2nd Applied Aerodynamics Conference, Seattle, WA, August 21-23, 1984.

32.Tavella, D., Wood, N., Harrits, P.: *Measurements on Wing-Tip Blowing*, Joint Institute for Aeronautics and Acoustics Paper JIAA TR-64, June 1985.

33.Tavella, D., Roberts, L.: *A Theory for Lateral Wing-Tip Blowing*, Joint Institute for Aeronautics and Acoustics Paper JIAA TR-60, June 1985.

34.Tavella, D., Roberts, L.: *The Concept of Lateral Blowing*, AIAA Paper 85-5000, AIAA 3rd Applied Aerodynamics Conference, Colorado Springs, CO, October 14-16, 1985.

35.Tavella, D., Lee, C.S., Wood, N.: *Influence of Wing Tip Configuration on Lateral Blowing Efficiency*, AIAA Paper 86-0475, AIAA 24th Aerospace Sciences Meeting, Reno, NV, January 6-9, 1986.

36.Smith, J.W., Mineck, R.E., Neuhart, D.H.: *Flow Visualization Studies of Blowing From the Tip of a Swept Wing*, NASA TM 4217, November 1990.

37.Mineck, R.E.: *Assessment of Potential Aerodynamic Benefits from Spanwise Blowing at the Wing Tip*, Ph.D. Dissertation, The George Washington University, May 1992.

38.Krist, S.L., Biedron, R.T., Rumsey, C.L.: *CFL3D User's Manual (Version 5.0)*, NASA TM-1998-208444, June 1998.

39.Roach, P.J.: *Verification and Validation in Computational Science and Engineering*, Hermosa Publishers, Albuquerque, NM, 1998.

40.Anderson, E.A., Snyder, D.S., Wright, C.T., Spall, R.E.: *Numerical/Experimental Investigation Into Multiple Vortex Structures Formed over Wings with Flat End-Caps*, AIAA Paper 2001-0112, 39th AIAA Aerospace Sciences Meeting, Reno, NV, January 8-11, 2001.

41.Francis, M.S., Kennedy, D.A.: *Formation of a Trailed Vortex*, Journal of Aircraft, Vol. 16, No. 3, March 1979, pp148-154.

11. Figures

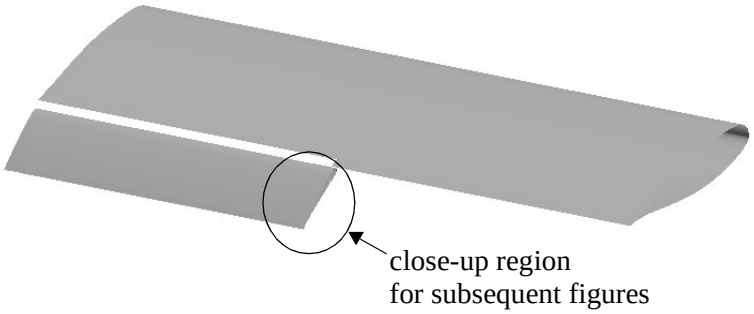

Figure 1: Baseline geometry.

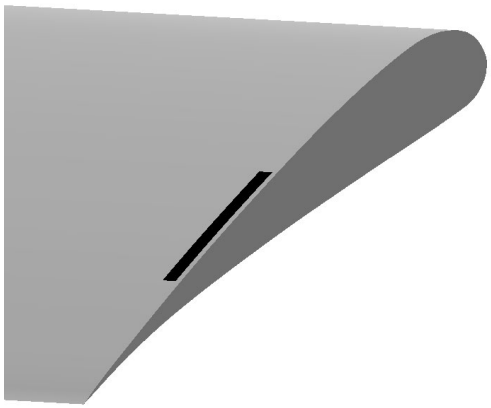

Figure 2: Close-up of flap with top blowing (configuration 1).

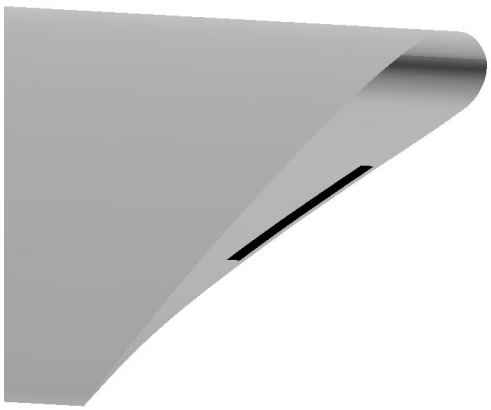

Figure 3: Close-up of flap with bottom blowing (configuration 2).

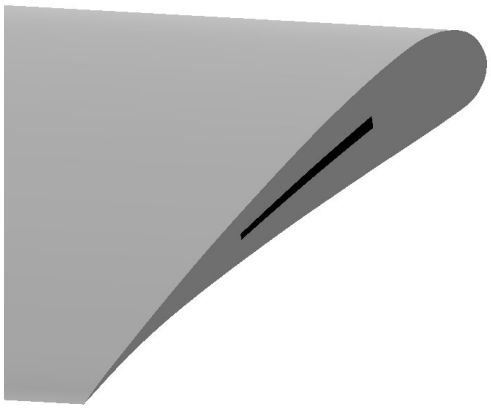

Figure 4: Close-up of flap with side blowing (configuration 3).

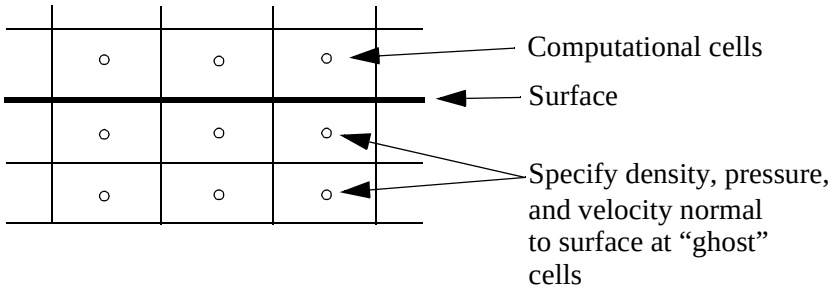

Figure 5: Schematic of new boundary condition.

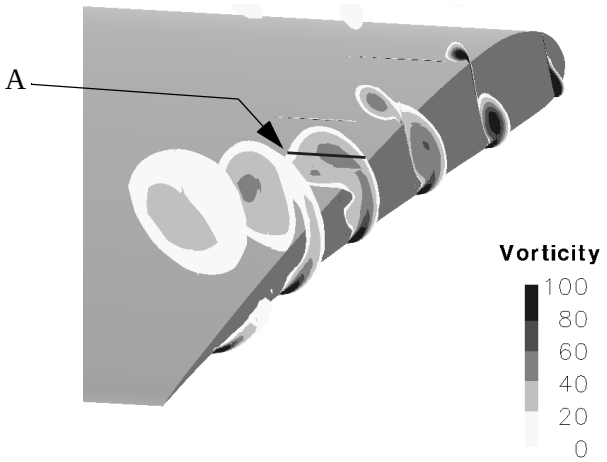

Figure 6: Baseline vorticity contours.

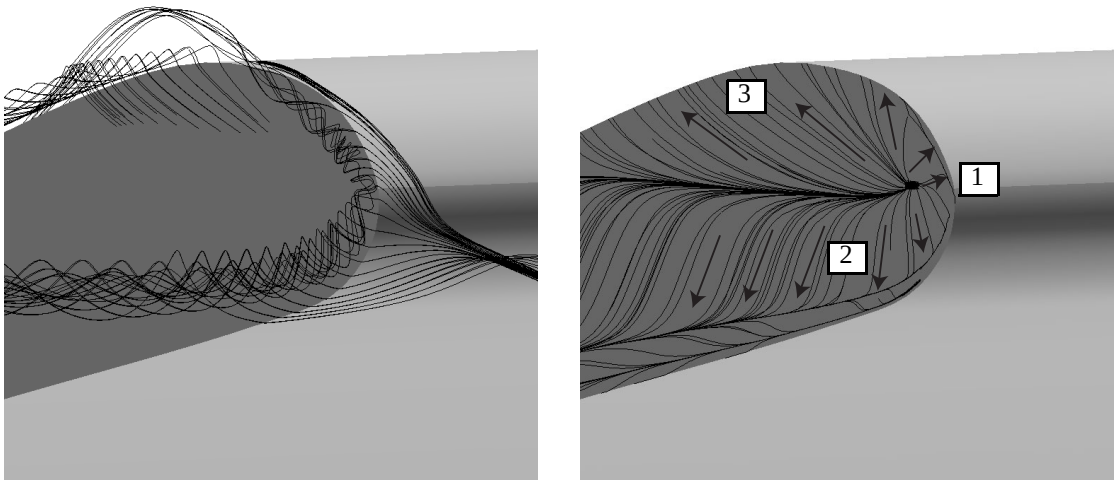

(a) Streamlines (b) Surface Flow

Figure 7: Baseline flap side edge flow: (a) streamlines and (b) surface flow.

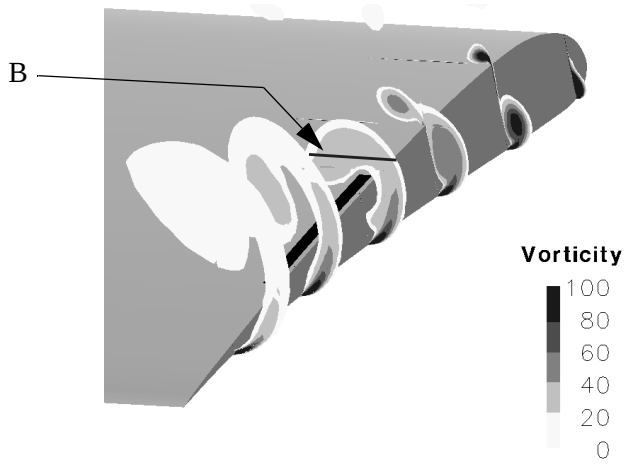

Figure 8: Configuration 1 vorticity contours.

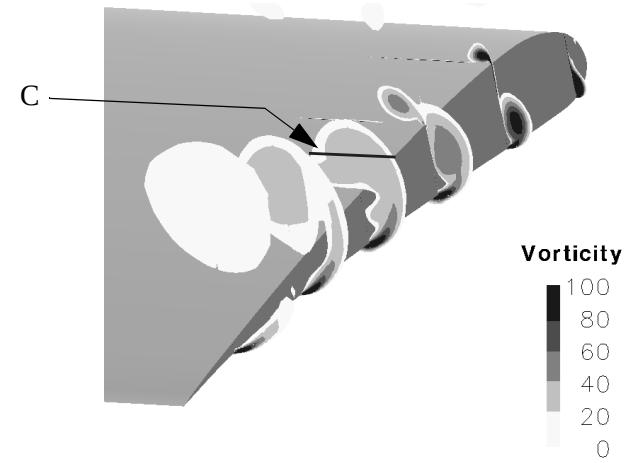

Figure 9: Configuration 2 vorticity contours.

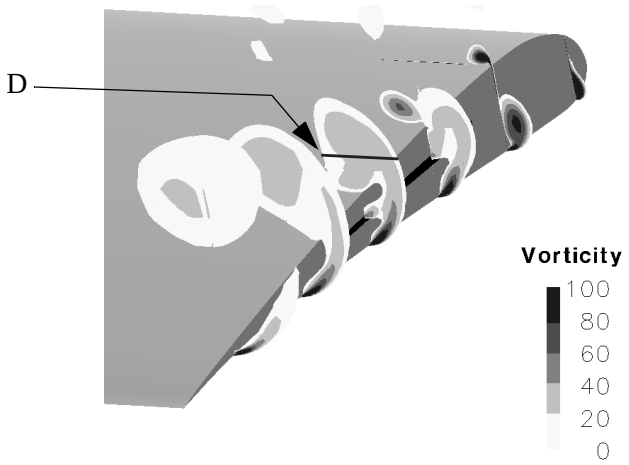

Figure 10: Configuration 3 vorticity contours.

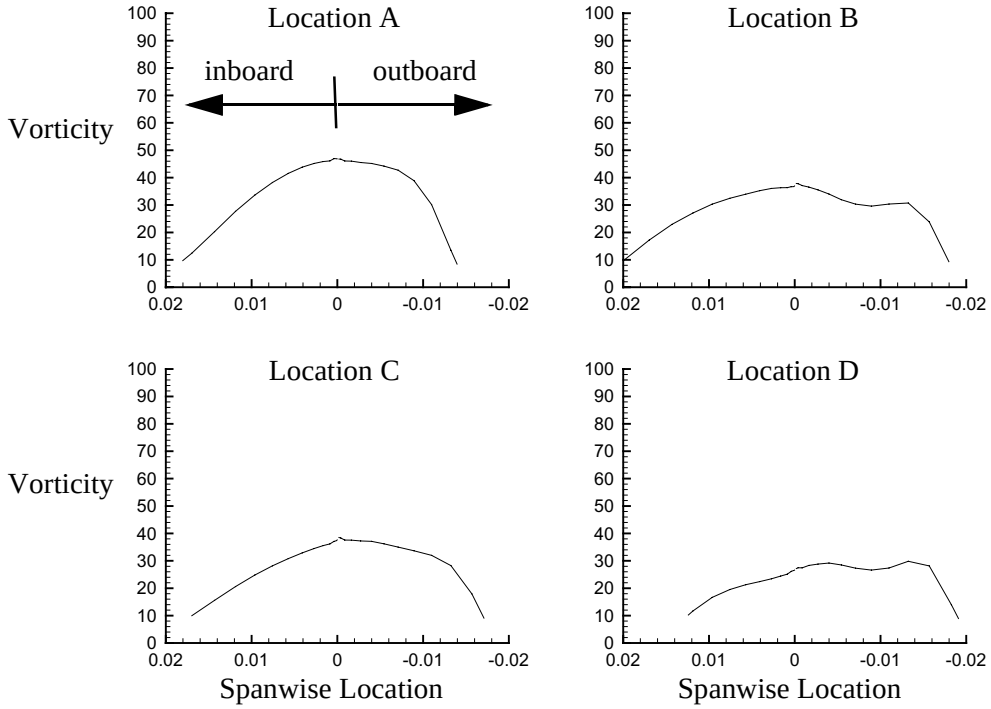

Figure 11: Normalized vorticity magnitude normal to the plane of the fourth slice for each case. Spanwise Location is normalized by the main element chord. Spanwise location = 0 is at the flap side edge.

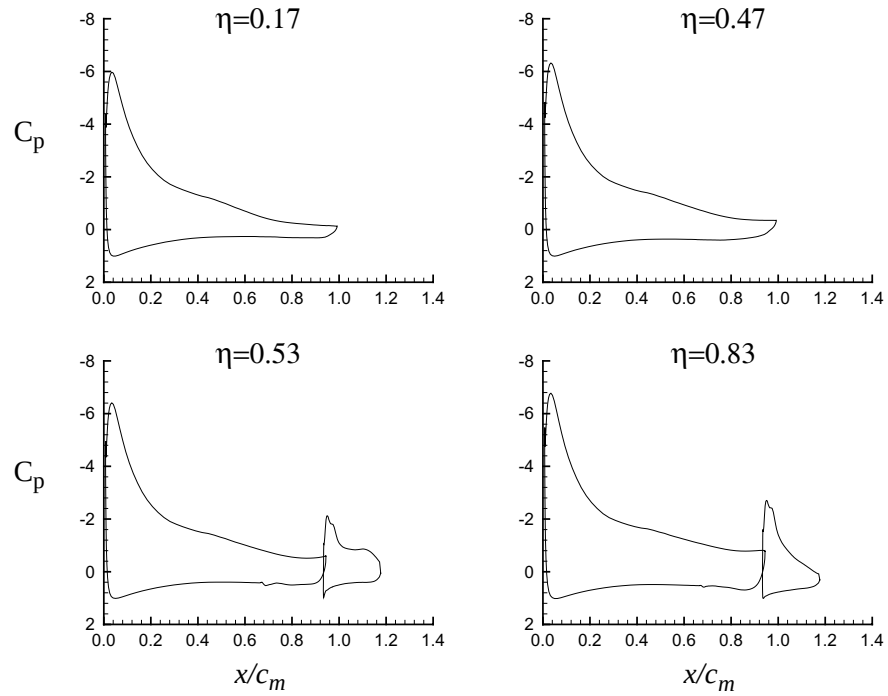

Figure 12: Baseline pressure coefficients at various spanwise locations.

REPORT DOCUMENTATION PAGE

Form Approved
OMB No. 0704-0188

1. REPORT DATE *(DD-MM-YYYY)*	2. REPORT TYPE	3. DATES COVERED *(From - To)*
01- 03 - 2005	Technical Memorandum	

4. TITLE AND SUBTITLE

Navier-Stokes Computations of a Wing-Flap Model With Blowing Normal to the Flap Surface

5a. CONTRACT NUMBER

5b. GRANT NUMBER

5c. PROGRAM ELEMENT NUMBER

6. AUTHOR(S)

Boyd, D. Douglas, Jr.

5d. PROJECT NUMBER

5e. TASK NUMBER

5f. WORK UNIT NUMBER

781-10-11-01

7. PERFORMING ORGANIZATION NAME(S) AND ADDRESS(ES)

NASA Langley Research Center
Hampton, VA 23681-2199

8. PERFORMING ORGANIZATION REPORT NUMBER

L-19072

9. SPONSORING/MONITORING AGENCY NAME(S) AND ADDRESS(ES)

National Aeronautics and Space Administration
Washington, DC 20546-0001

10. SPONSOR/MONITOR'S ACRONYM(S)

NASA

11. SPONSOR/MONITOR'S REPORT NUMBER(S)

NASA/TM-2005-213542

12. DISTRIBUTION/AVAILABILITY STATEMENT

Unclassified - Unlimited
Subject Category 71
Availability: NASA CASI (301) 621-0390

13. SUPPLEMENTARY NOTES

Supersedes NASA internal report CDTM-10039
An electronic version can be found at http://ntrs.nasa.gov

14. ABSTRACT

A computational study of a generic wing with a half span flap shows the mean flow effects of several blown flap configurations. The effort compares and contrasts the thin-layer, Reynolds averaged, Navier-Stokes solutions of a baseline wing-flap configuration with configurations that have blowing normal to the flap surface through small slits near the flap side edge. Vorticity contours reveal a dual vortex structure at the flap side edge for all cases. The dual vortex merges into a single vortex at approximately the mid-flap chord location. Upper surface blowing reduces the strength of the merged vortex and moves the vortex away from the upper edge. Lower surface blowing thickens the lower shear layer and weakens the merged vortex, but not as much as upper surface blowing. Side surface blowing forces the lower surface vortex farther outboard of the flap edge by effectively increasing the aerodynamic span of the flap. It is seen that there is no global aerodynamic penalty or benefit from the particular blowing configurations examined.

15. SUBJECT TERMS

Internally blown flap; Flap surface blowing; Multi-element airfoil; Computational Fluid Dynamics (CFD)

16. SECURITY CLASSIFICATION OF:			17. LIMITATION OF ABSTRACT	18. NUMBER OF PAGES	19a. NAME OF RESPONSIBLE PERSON
a. REPORT	b. ABSTRACT	c. THIS PAGE			STI Help Desk (email: help@sti.nasa.gov)
					19b. TELEPHONE NUMBER *(Include area code)*
U	U	U	UU	24	(301) 621-0390